

# Diamagnetism and suppression of screening as hallmarks of electron-hole pairing in a double layer graphene system

K. V. Germash, D. V. Fil

*Institute for Single Crystals, National Academy of Sciences of Ukraine, Lenin Ave. 60, Kharkov 61001, Ukraine*

We study how the electron-hole pairing reveals itself in the response of a double layer graphene system to the vector and scalar potentials. Electron-hole pairing results in a rigid (London) relation between the current and the difference of vector potentials in two adjacent layers. The diamagnetic effect can be observed in multiple connected systems in the magnetic field parallel to the graphene layers. Such an effect would be considered as a hallmark of the electron-hole pairing, but the value of the effect is extremely small. Electron-hole pairing significantly changes the response to the scalar potential, as well. It results in a complete (at zero temperature) or partial (at finite temperature) suppression of screening of the electric field of a test charge situated at some distance to the double layer system. A strong increase of the electric field induced by the test charge under decrease in temperature can be considered as a spectacular hallmark of the electron-hole pairing.

PACS numbers: 71.35.Lk; 73.22.Pr; 74.20.-z

## I. INTRODUCTION

The idea to realize the electron-hole pairing and the counterflow superconductivity in adjacent electron-doped and hole-doped conducting layers was put forward in Refs. 1,2. Electron-hole pairs with spatially separated components may provide a flow of equal in modulus and oppositely directed electrical currents in the double layer system. The transition of the gas of such pairs into the superfluid state can be considered as a kind of the superconductive transition.

The electron-hole pairing was also predicted for the quantum Hall bilayers<sup>3-5</sup> with the total filling factor of Landau levels  $\nu_1 + \nu_2 = 1$  ( $\nu_i$  is the filling factor of the  $i$ th layer). In the latter systems empty states in the zeroth Landau level play the role of holes. The electron-hole pairing in quantum Hall bilayers was observed experimentally. The pairing results in the exponential increase of the counterflow conductivity<sup>6-8</sup>, and the negative perfect interlayer drag<sup>9</sup> at low ( $T < 0.1$  K) temperature.

The idea to realize electron-hole pairing in a double layer graphene system was put forward in Refs. 10–12. In graphene the electron and hole Fermi circles are nested at equal densities of carriers, which is the favorable condition for the electron-hole pairing. In addition, the type of carriers (electrons or holes) and their densities can be easily controlled by external gates. The estimate for the critical temperature given in Ref. 11 is very optimistic ( $T_c \approx 300$  K).

It was shown<sup>13</sup> that screening may significantly (in six orders) reduce the critical temperature. The pessimistic conclusion<sup>13</sup> was put in question in Refs. 14,15. The electron-hole pairing suppresses screening and the problem should be treated self-consistently. If the bare coupling constant is quite large, the influence of screening on the critical temperature is not so crucial. Using a self-consistent treatment of dynamic screening, the authors of Ref. 14 have shown that at sufficiently small interlayer distance the excitonic gap (the order parameter for the electron-hole pairing) can reach values of the order of the Fermi energy. In that case the critical temperature can be rather large (up to 100 K).

It was predicted<sup>16</sup> that the counterflow superconductivity at high temperature can also be observed in a pair of adjacent bilayer graphene sheets. The advantage of the latter system is that the coupling parameter depends on the density of carriers and this parameter can be controlled by external gates. Using few-layer ABC stacked sheets of graphene instead of monolayer or bilayer graphene sheets one may further increase the critical temperature<sup>17</sup>. The increasing is caused by the enhancing of the density of states in the few-layer graphene.

Drag experiments support the idea of the electron-hole pairing in electron-hole double layer systems in zero magnetic field. An anomalous increase in the drag resistance at low temperature was observed in GaAs-AlGaAs double quantum well heterostructures at small ( $< 20$  nm) interlayer distances<sup>18,19</sup>. The effect is larger in samples with lower density of the carrier. The anomalous drag was registered in a hybrid double layer system comprising a single-layer (or bilayer) graphene in close proximity to a quantum well created in GaAs<sup>20</sup>. In the latter system the value of the anomalous drag is larger than in the GaAs double layer structures<sup>18,19</sup> and the effect is registered at higher temperature. At the same time, the double layer graphene system<sup>21</sup> does not show any low temperature increase in the drag resistance down to the temperature about 1 K. The anomalous drag can be explained by the electron-hole pairing. The experimental situation correlates to the understanding<sup>14-16</sup> that the critical temperature is very sensitive to the parameters of the double layer system (the electron spectrum, the interlayer distance, the density of the carriers, etc.).

Generally, the transition into the superconductive state is registered not only in transport measurements, but in

magnetic measurements, as well. The Meissner effect is a known indicator of the superconductive transition. This indicator is especially important in a situation where only a partial lowering of the resistance is observed (when only part of the sample is superconductive). The Meissner effect can be derived from the London equation. In the case of the counterflow superconductivity the London equation (its analog) determines the rigid relation between the counterflow current and the difference of the vector potentials in graphene sheets. The system demonstrates the diamagnetic response to the magnetic field directed parallel to the layers. The effect can be observed in a multiple-connected geometry. The density of the induced current can be rather large, but the diamagnetic effect is extremely small.

For the electron-hole pairing the counterpart of the Meissner effect is the suppression of screening. The response to the difference of the vector potentials in the layers is similar to the response to the sum of the scalar potentials. The suppression of screening is specific for the counterflow superconductivity. Screening is connected with the appearance of the induced charges in the conducting layers. In the case of the electron-hole pairing the positive and negative induced charges are correlated, which reduces screening. We propose to observe the suppression of screening by the measurement of the electrostatic field of a test charge located near the graphene sheets. We show that at zero temperature screening should be completely suppressed at large distance to the test charge. At finite temperatures much lower than the critical temperature the suppression is strong but partial. This behavior can be considered as a spectacular hallmark of the electron-hole pairing.

## II. DENSITY AND CURRENT OPERATORS FOR THE MONOLAYER AND BILAYER GRAPHENE

For computing the density-density and the current-current response functions we need the explicit expressions for the density operator and the current operator. For graphene these operators differ from those for a free electron gas with the quadratic spectrum. In this section we derive the expressions for the Fourier component of the density and the current operator for the monolayer and the bilayer graphene.

The Hamiltonian that describes low-energy electrons in the monolayer and bilayer graphene has the form<sup>22</sup>

$$\begin{aligned}
 H_m &= \hbar v_F \begin{pmatrix} 0 & \hat{k}_x - i\hat{k}_y & 0 & 0 \\ \hat{k}_x + i\hat{k}_y & 0 & 0 & 0 \\ 0 & 0 & 0 & \hat{k}_x + i\hat{k}_y \\ 0 & 0 & \hat{k}_x - i\hat{k}_y & 0 \end{pmatrix} \otimes \mathbf{1}_\sigma, \\
 H_b &= -\frac{\hbar^2}{2m} \begin{pmatrix} 0 & (\hat{k}_x - i\hat{k}_y)^2 & 0 & 0 \\ (\hat{k}_x + i\hat{k}_y)^2 & 0 & 0 & 0 \\ 0 & 0 & 0 & (\hat{k}_x + i\hat{k}_y)^2 \\ 0 & 0 & (\hat{k}_x - i\hat{k}_y)^2 & 0 \end{pmatrix} \otimes \mathbf{1}_\sigma,
 \end{aligned} \tag{1}$$

where  $\hat{\mathbf{k}} = -i\nabla$  is the wave number operator,  $\mathbf{1}_\sigma$  is unit matrix that acts in the spin space,  $v_F$  is the Fermi velocity for the monolayer graphene and  $m$  is the effective mass for the bilayer graphene. The two latter quantities are the material parameters:  $v_F \approx 10^8$  cm/s, and  $m \approx 0.03m_e$ , where  $m_e$  is the free electron mass. Here and below the index  $m(b)$  corresponds to the monolayer (bilayer) graphene.

The Hamiltonian (1) acts in the space of the eight-component vectors

$$\Phi = \begin{pmatrix} \Psi_{K\uparrow} \\ \Psi_{K'\uparrow} \\ \Psi_{K\downarrow} \\ \Psi_{K'\downarrow} \end{pmatrix}, \tag{2}$$

where

$$\Psi_{K\sigma} = \begin{pmatrix} \Psi_A \\ \Psi_B \end{pmatrix} \tag{3}$$

is the pseudospinor whose components correspond to different graphene sublattices (labeled as  $A$  and  $B$ ),  $K(K')$  is the valley index, and  $\sigma$  is the spin index.

Since the Hamiltonian (1) is diagonal in the valley and spin indexes, the pure spin-valley states described by the spinor (3) are the eigenvectors of (1). For the pure state the vector (2) contains only one nonzero component  $\Psi_{K\sigma}$ . The eigenvalues and the eigenfunctions for the pure states are

$$\varepsilon_{\lambda,\mathbf{k}}^m = \lambda \hbar v_F k, \quad \Psi_{\alpha,\sigma,\lambda,\mathbf{k}}^{(m)}(\mathbf{r}) = \frac{e^{i\mathbf{k}\mathbf{r}}}{\sqrt{2S}} \begin{pmatrix} e^{-i\alpha\frac{\theta_{\mathbf{k}}}{2}} \\ \lambda e^{i\alpha\frac{\theta_{\mathbf{k}}}{2}} \end{pmatrix}, \tag{4}$$

$$\varepsilon_{\lambda,\mathbf{k}}^b = \lambda \frac{\hbar^2 k^2}{2m_b}, \quad \Psi_{\alpha,\sigma,\lambda,\mathbf{k}}^{(b)}(\mathbf{r}) = \frac{e^{i\mathbf{k}\mathbf{r}}}{\sqrt{2S}} \begin{pmatrix} e^{-i\alpha\theta_{\mathbf{k}}} \\ -\lambda e^{i\alpha\theta_{\mathbf{k}}} \end{pmatrix}, \quad (5)$$

where  $\alpha = \pm 1$  corresponds to the  $K(K')$  valley, and  $\lambda = \pm 1$  corresponds to the conductive (valence) subband. In (4) and (5)  $\theta_{\mathbf{k}}$  is the angle between the vector  $\mathbf{k}$  and the  $x$  axis, and  $S$  is the area of the system. We note that due to the spin-valley degeneracy the superposition of four pure states with the same  $\mathbf{k}$  and  $\lambda$  is also the eigenvector of (1).

The operator of the creation (annihilation) of an electron at the coordinate  $\mathbf{r}$  can be expressed through the operators of the creation (annihilation) of an electron in the eigenstate with given  $\lambda$  and  $\mathbf{k}$ :

$$\Psi^+(\mathbf{r}) = \sum_{\alpha,\sigma,\lambda,\mathbf{k}} \Phi_{\alpha,\sigma,\lambda,\mathbf{k}}^+(\mathbf{r}) c_{\alpha,\sigma,\lambda,\mathbf{k}}^+, \quad \Psi(\mathbf{r}) = \sum_{\alpha,\sigma,\lambda,\mathbf{k}} \Phi_{\alpha,\sigma,\lambda,\mathbf{k}}(\mathbf{r}) c_{\alpha,\sigma,\lambda,\mathbf{k}}. \quad (6)$$

In the second quantization representation the Hamiltonian (1) is diagonal in  $c_{\alpha,\sigma,\lambda,\mathbf{k}}$  operators:

$$H = \sum_{\sigma,\alpha,\lambda,\mathbf{k}} \varepsilon_{\lambda,\mathbf{k}} c_{\sigma,\alpha,\lambda,\mathbf{k}}^+ c_{\sigma,\alpha,\lambda,\mathbf{k}}. \quad (7)$$

From (6) we obtain the Fourier component of the density operator for the monolayer (bilayer) graphene:

$$\begin{aligned} \rho^{m(b)}(\mathbf{q}) &= \sum_{\alpha,\sigma,\lambda,\mathbf{k},\alpha',\sigma',\lambda',\mathbf{k}'} \int d\mathbf{r} e^{i\mathbf{q}\mathbf{r}} \Phi_{\alpha',\sigma',\lambda',\mathbf{k}'}^+(\mathbf{r}) \Phi_{\alpha,\sigma,\lambda,\mathbf{k}}(\mathbf{r}) c_{\alpha',\sigma',\lambda',\mathbf{k}'}^+ c_{\alpha,\sigma,\lambda,\mathbf{k}} \\ &= \sum_{\alpha,\sigma,\lambda,\lambda',\mathbf{k}} f_{\alpha,\lambda,\lambda',\mathbf{k},\mathbf{q}}^{m(b)} c_{\alpha,\sigma,\lambda',\mathbf{k}+\mathbf{q}}^+ c_{\alpha,\sigma,\lambda,\mathbf{k}}, \end{aligned} \quad (8)$$

where

$$f_{\alpha,\lambda,\lambda',\mathbf{k},\mathbf{q}}^m = \frac{e^{i\alpha\frac{\theta_{\mathbf{k}+\mathbf{q}}-\theta_{\mathbf{k}}}{2}} + \lambda\lambda' e^{-i\alpha\frac{\theta_{\mathbf{k}+\mathbf{q}}-\theta_{\mathbf{k}}}{2}}}{2} \quad (9)$$

and

$$f_{\alpha,\lambda,\lambda',\mathbf{k},\mathbf{q}}^b = \frac{e^{i\alpha(\theta_{\mathbf{k}+\mathbf{q}}-\theta_{\mathbf{k}})} + \lambda\lambda' e^{-i\alpha(\theta_{\mathbf{k}+\mathbf{q}}-\theta_{\mathbf{k}})}}{2}. \quad (10)$$

Note that the density operator (8) contains the diagonal as well as off-diagonal in  $\lambda$  terms. In other words, the density operator cannot be presented as a sum of the valence band and the conductive band density operators.

To obtain the operator of the current we replace the wave number operator  $\hat{\mathbf{k}}$  in the Hamiltonian (1) with the gauge invariant operator  $\hat{\mathbf{k}} - (e/\hbar c)\mathbf{A}$  ( $c$  is the light velocity) and consider a variation of the Hamiltonian under the variation in the vector potential  $\mathbf{A}$ . The current operator is given by the equation

$$\hat{\mathbf{j}}(\mathbf{r}) = -c\Psi^+(\mathbf{r}) \frac{\delta H}{\delta \mathbf{A}} \Psi(\mathbf{r}). \quad (11)$$

For the monolayer graphene the Fourier component of the operator (11) is presented in the form

$$\hat{\mathbf{j}}^m(\mathbf{q}) = ev_F \sum_{\alpha,\sigma,\lambda,\lambda',\mathbf{k}} \mathbf{g}_{\alpha,\lambda,\lambda',\mathbf{k},\mathbf{q}}^m c_{\alpha,\sigma,\lambda',\mathbf{k}+\mathbf{q}}^+ c_{\alpha,\sigma,\lambda,\mathbf{k}}, \quad (12)$$

where  $\mathbf{g}^m = g_x^m \mathbf{i}_x + g_y^m \mathbf{i}_y$ ,  $\mathbf{i}_x$  and  $\mathbf{i}_y$  are the unit vectors along the  $x$  and  $y$  axes, and

$$\begin{aligned} g_x^m &= \frac{\lambda e^{i\alpha\frac{\theta_{\mathbf{k}+\mathbf{q}}+\theta_{\mathbf{k}}}{2}} + \lambda' e^{-i\alpha\frac{\theta_{\mathbf{k}+\mathbf{q}}+\theta_{\mathbf{k}}}{2}}}{2}, \\ g_y^m &= -i\alpha \frac{\lambda e^{i\alpha\frac{\theta_{\mathbf{k}+\mathbf{q}}+\theta_{\mathbf{k}}}{2}} - \lambda' e^{-i\alpha\frac{\theta_{\mathbf{k}+\mathbf{q}}+\theta_{\mathbf{k}}}{2}}}{2}. \end{aligned} \quad (13)$$

We note that the current operator (12) does not contain the diamagnetic term (the term proportional to  $\mathbf{A}$ ), different from the current operator for a free electron gas.

Repeating the same procedure for the bilayer graphene we obtain

$$\hat{j}_x^b(\mathbf{q}) = \frac{e\hbar}{m} \sum_{\alpha,\sigma,\lambda,\lambda',\mathbf{k}} \left[ \left( k_x + \frac{q_x}{2} - \frac{e}{\hbar c} A_x \right) g_x^b + \left( k_y + \frac{q_y}{2} - \frac{e}{\hbar c} A_y \right) g_y^b \right] c_{\alpha,\sigma,\lambda',\mathbf{k}+\mathbf{q}}^+ c_{\alpha,\sigma,\lambda,\mathbf{k}}, \quad (14)$$

$$\hat{j}_y^b(\mathbf{q}) = \frac{e\hbar}{m} \sum_{\alpha,\sigma,\lambda,\lambda',\mathbf{k}} \left[ \left( k_x + \frac{q_x}{2} - \frac{e}{\hbar c} A_x \right) g_y^b - \left( k_y + \frac{q_y}{2} - \frac{e}{\hbar c} A_y \right) g_x^b \right] c_{\alpha,\sigma,\lambda',\mathbf{k}+\mathbf{q}}^+ c_{\alpha,\sigma,\lambda,\mathbf{k}}, \quad (15)$$

where

$$\begin{aligned} g_x^b &= \frac{\lambda e^{i\alpha(\theta_{\mathbf{k}+\mathbf{q}}+\theta_{\mathbf{k}})} + \lambda' e^{-i\alpha(\theta_{\mathbf{k}+\mathbf{q}}+\theta_{\mathbf{k}})}}{2}, \\ g_y^b &= -i\alpha \frac{\lambda e^{i\alpha(\theta_{\mathbf{k}+\mathbf{q}}+\theta_{\mathbf{k}})} - \lambda' e^{-i\alpha(\theta_{\mathbf{k}+\mathbf{q}}+\theta_{\mathbf{k}})}}{2}. \end{aligned} \quad (16)$$

Formally, the operator  $\hat{j}^b$  contains the diamagnetic term, but in fact, due to the factors  $g_x^b$  and  $g_y^b$  this term does not contribute to the current after the averaging over the angle.

### III. DOUBLE LAYER GRAPHENE SYSTEM IN THE NAMBU REPRESENTATION

Let us now consider the double layer system made of two graphene sheets. The graphene sheet 1 is assumed to be the electron doped and the graphene sheet 2, the hole doped. The density of electrons is equal to the density of holes. The Hamiltonian of the system has the form

$$H = \sum_{i=1,2} \sum_{\sigma,\alpha} \sum_{\lambda,\mathbf{k}} (\varepsilon_{\lambda,\mathbf{k}} - \epsilon_{F,i}) c_{i,\sigma,\alpha,\lambda,\mathbf{k}}^+ c_{i,\sigma,\alpha,\lambda,\mathbf{k}} + H_{int}, \quad (17)$$

where  $i$  is the layer index, and  $\epsilon_{F,1} = +\epsilon_F$ ,  $\epsilon_{F,2} = -\epsilon_F$  are the Fermi energies. The Hamiltonian  $H_{int}$  includes the intralayer and interlayer Coulomb interaction

$$H_{int} = \frac{1}{2S} \sum_{i,j=1,2} \sum_{\mathbf{q}} V_{ij}(q) : \hat{\rho}_i(\mathbf{q}) \hat{\rho}_j(-\mathbf{q}) :, \quad (18)$$

where  $V_{ij}(q)$  are the Fourier components of the interaction potential, and the notation  $: \hat{\rho} \hat{\rho} :$  means the normal ordering.

In the system with the electron-hole pairing the average  $\langle c_{1,\lambda,\mathbf{k}}^+ h_{2,-\lambda,-\mathbf{k}}^+ \rangle$  (where  $h^+$  is the hole creation operator in layer 2) is nonzero. Taking into account that  $h_{2,-\lambda,-\mathbf{k}}^+ = c_{2,\lambda,\mathbf{k}}$  the pairing can be equivalently described in terms of  $\langle c_{1,\lambda,\mathbf{k}}^+ c_{2,-\lambda,\mathbf{k}} \rangle$  averages.

The mean-field Hamiltonian can be presented in the matrix form that is the analog of the Nambu representation

$$H_{MF} = \sum_{\sigma,\alpha} \sum_{\mathbf{k},\lambda} \hat{C}_{\lambda,\mathbf{k}}^+ \hat{\epsilon}_{\lambda,\mathbf{k}} \hat{C}_{\lambda,\mathbf{k}}, \quad (19)$$

where

$$\hat{C}_{\lambda,\mathbf{k}} = \begin{pmatrix} c_{1,\sigma,\alpha,\lambda,\mathbf{k}} \\ c_{2,\sigma,\alpha,-\lambda,\mathbf{k}} \end{pmatrix}, \quad \hat{C}_{\lambda,\mathbf{k}}^+ = ( c_{1,\sigma,\alpha,\lambda,\mathbf{k}}^+ \quad c_{2,\sigma,\alpha,-\lambda,\mathbf{k}}^+ ) \quad (20)$$

and

$$\hat{\epsilon}_{\lambda,\mathbf{k}} = \xi_{\lambda,\mathbf{k}} \hat{\tau}_3 - \Delta_{\lambda,\mathbf{k}} \hat{\tau}_1 \quad (21)$$

with  $\xi_{\lambda,\mathbf{k}} = \varepsilon_{\lambda,\mathbf{k}}^{m(b)} - \epsilon_F$ . Here  $\hat{\tau}_i$  are the Pauli matrices. Since Eqs. (19) and (21) are the same as in the original Nambu approach<sup>23</sup> one can use the standard diagram technique for obtaining the response functions.

The interaction part of the Hamiltonian  $H'_{int} = H - H_{MF}$  determines the self-energy contribution to the spectrum. The condition for this contribution not to renormalize  $\Delta_{\lambda,\mathbf{k}}$  yields the self-consistence equation

$$\Delta_{\lambda,\mathbf{k}} = \sum_{\lambda',\mathbf{q}} V_{12}^{scr}(q) F_{\lambda,\lambda',\mathbf{k},\mathbf{q}}^{m(b)} \frac{\Delta_{\lambda',\mathbf{k}+\mathbf{q}}}{2E_{\lambda',\mathbf{k}+\mathbf{q}}} \tanh \frac{E_{\lambda',\mathbf{k}+\mathbf{q}}}{2T}, \quad (22)$$

where  $E_{\lambda,\mathbf{k}} = \sqrt{\xi_{\lambda,\mathbf{k}}^2 + \Delta_{\lambda,\mathbf{k}}^2}$  is the energy spectrum,

$$F_{\lambda,\lambda',\mathbf{k},\mathbf{q}}^m = \frac{1 + \lambda\lambda' \cos(\theta_{\mathbf{k}+\mathbf{q}} - \theta_{\mathbf{k}})}{2}, \quad F_{\lambda,\lambda',\mathbf{k},\mathbf{q}}^b = \frac{1 + \lambda\lambda' \cos[2(\theta_{\mathbf{k}+\mathbf{q}} - \theta_{\mathbf{k}})]}{2}, \quad (23)$$

and  $V_{12}^{scr}(q)$  is the potential of screened interlayer Coulomb interaction. For obtaining this potential one can use the random phase approximation. In the general case this approximation yields the frequency dependent potential  $V_{12}^{scr}(q, \omega)$ . In (22)  $V_{12}^{scr}(q) = V_{12}^{scr}(q, 0)$  (the static screening approximation). This approximation overestimates the influence of screening on the electron-hole pairing<sup>14</sup>. Using the dynamical screening approximation for the system of two suspended monolayer graphene sheets the authors of Ref. 14 have shown that the self-consistence equation has the solution  $\Delta_{\lambda, \mathbf{k}} \sim \epsilon_F$  if the interlayer distance is small enough. Applying the dynamical screening approach to the system of two suspended bilayer graphene sheets we arrive at the same conclusion. We will not present here the details. Our starting point is that under the appropriate conditions the electron-hole pairing takes place in a system of two monolayer or two bilayer graphene sheets at rather high temperatures and in this case the order parameter of the electron-hole pairing  $\Delta_{\lambda, \mathbf{k}}$  is comparable in value with the Fermi energy.

In the Nambu representation the density operators can be presented in the following compact form:

$$\hat{\rho}_+(\mathbf{q}) = \hat{\rho}_1(\mathbf{q}) + \hat{\rho}_2(\mathbf{q}) = \sum_{\alpha, \sigma, \lambda, \lambda', \mathbf{k}} f_{\alpha, \lambda, \lambda', \mathbf{k}, \mathbf{q}}^{m(b)} \hat{C}_{\lambda', \mathbf{k}+\mathbf{q}}^+ \tau_0 \hat{C}_{\lambda, \mathbf{k}}, \quad (24)$$

$$\hat{\rho}_-(\mathbf{q}) = \hat{\rho}_1(\mathbf{q}) - \hat{\rho}_2(\mathbf{q}) = \sum_{\alpha, \sigma, \lambda, \lambda', \mathbf{k}} f_{\alpha, \lambda, \lambda', \mathbf{k}, \mathbf{q}}^{m(b)} \hat{C}_{\lambda', \mathbf{k}+\mathbf{q}}^+ \tau_3 \hat{C}_{\lambda, \mathbf{k}}, \quad (25)$$

where  $\tau_0$  is the identity matrix.

The current operators for the system of two monolayer graphenes can be written as

$$\hat{\mathbf{j}}_+(\mathbf{q}) = \hat{\mathbf{j}}_1(\mathbf{q}) + \hat{\mathbf{j}}_2(\mathbf{q}) = ev_F \sum_{\alpha, \sigma, \lambda, \lambda', \mathbf{k}} \mathbf{g}_{\alpha, \lambda, \lambda', \mathbf{k}, \mathbf{q}}^m \hat{C}_{\lambda', \mathbf{k}+\mathbf{q}}^+ \tau_3 \hat{C}_{\lambda, \mathbf{k}}, \quad (26)$$

$$\hat{\mathbf{j}}_-(\mathbf{q}) = \hat{\mathbf{j}}_1(\mathbf{q}) - \hat{\mathbf{j}}_2(\mathbf{q}) = ev_F \sum_{\alpha, \sigma, \lambda, \lambda', \mathbf{k}} \mathbf{g}_{\alpha, \lambda, \lambda', \mathbf{k}, \mathbf{q}}^m \hat{C}_{\lambda', \mathbf{k}+\mathbf{q}}^+ \tau_0 \hat{C}_{\lambda, \mathbf{k}}. \quad (27)$$

The important feature of (26),(27) and (24),(25) is that the operator  $\hat{\rho}_+$  contains the same matrix ( $\tau_0$ ) as the operator  $\hat{\mathbf{j}}_-$ . It reflects the connection between the Meissner effect and the suppression of screening. The Meissner effect is determined by the behavior of the  $\hat{\mathbf{j}}_-$  response function. In its turn, the screening at large distances is determined by the behavior of the  $\rho_+$  response function.

Here we do not present the expression for  $\hat{\mathbf{j}}_{\pm}$  for the system of two bilayer graphenes. These expressions are just the straightforward generalization of (14),(15) and (26),(27).

#### IV. LONDON EQUATION FOR THE COUNTERFLOW SUPERCONDUCTOR

Phenomenologically, the electron-hole pair can be described as a polar particle with the mass equal to the sum of the effective electron and hole masses  $M = m_e^* + m_h^*$ . Such a description works well for the double layer system with the quadratic spectrum of carriers<sup>24</sup>. The superfluid velocity  $\mathbf{v}_s$  for the Bose-Einstein condensate (quasicondensate) of such pairs is proportional to the gradient of the phase of the condensate wave function:  $\mathbf{v}_s = (\hbar/M)\nabla\varphi$ . The electric currents connected with the flow of electron-hole pairs are

$$\mathbf{j}_1 = -\mathbf{j}_2 = en_s \mathbf{v}_s = \frac{e\hbar n_s}{M} \nabla\varphi, \quad (28)$$

where  $n_s$  is the superfluid density. At  $T = 0$  the superfluid density is equal to the electron (hole) density.

In the magnetic field the polar particles feel the effective vector potential proportional to the vector product of the magnetic field and the dipole moment of the particle  $\mathbf{p}$ :  $\mathbf{A}_{eff} = \mathbf{B} \times \mathbf{p}/e^{25,26}$ . For the planar system  $\mathbf{A}_{eff} = \mathbf{A}_{1,pl} - \mathbf{A}_{2,pl}$ , where  $\mathbf{A}_{i,pl}$  is the planar component of the vector potential in the  $i$ th plane. In this case the electric current is given by the equation

$$\mathbf{j}_1 = -\mathbf{j}_2 = \frac{e\hbar n_s}{M} \left[ \nabla\varphi - \frac{e}{\hbar c} (\mathbf{A}_{1,pl} - \mathbf{A}_{2,pl}) \right]. \quad (29)$$

Superfluid density is connected with another important quantity - the superfluid stiffness  $\rho_s$ . This quantity determines the temperature of the superfluid transition  $T_c$  in a two-dimensional nonideal Bose gas. The temperature  $T_c$  satisfies the equation<sup>27</sup>

$$T_c = \frac{\pi}{2} \rho_s(T_c) \quad (30)$$

( $\rho_s$  depends on the temperature). Superfluid stiffness is defined as the coefficient of expansion of the free energy in the phase gradient

$$F = F_0 + \frac{1}{2} \int d^2r \rho_s (\nabla\varphi)^2. \quad (31)$$

In the presence of the vector potential the phase gradient should be replaced with the gauge-invariant quantity  $\nabla\varphi - \frac{e}{\hbar c} \mathbf{A}_{eff}$ . The variation of the free energy with respect to the vector potential yields

$$\delta F = - \int d^2r \frac{e}{\hbar c} \rho_s \left[ \nabla\varphi - \frac{e}{\hbar c} (\mathbf{A}_{1,pl} - \mathbf{A}_{2,pl}) \right] (\delta \mathbf{A}_{1,pl} - \delta \mathbf{A}_{2,pl}). \quad (32)$$

On the other hand

$$\delta F = - \frac{1}{c} \int d^2r (\mathbf{j}_1 \delta \mathbf{A}_{1,pl} + \mathbf{j}_2 \delta \mathbf{A}_{2,pl}). \quad (33)$$

As follows from Eqs. (32) and (33), the superfluid stiffness is the coefficient of proportionality between the electric current and the gauge-invariant quantity  $(e/\hbar)[\nabla\varphi - (e/\hbar c)\mathbf{A}_{eff}]$ . In particular, at  $\nabla\varphi = 0$  we obtain

$$\mathbf{j}_- = \mathbf{j}_1 - \mathbf{j}_2 = - \frac{2e^2 \rho_s}{\hbar^2 c} (\mathbf{A}_{1,pl} - \mathbf{A}_{2,pl}). \quad (34)$$

Equation (34) can be considered as an analog of the London equation for the counterflow superconductor.

The phenomenological approach<sup>24</sup> yields the following expression for the superfluid stiffness:

$$\rho_s = \frac{\hbar^2 n_s}{M}. \quad (35)$$

The same expression appears in the microscopic theory of the electron-hole pairing<sup>1</sup>.

Since the mass of the carrier in the monolayer graphene is equal to zero, Eq. (35) cannot be applied to the system of two monolayer graphenes. To overcome this difficulty we take into account that the current can be found as a linear response to the vector potential. The superfluid stiffness can be obtained as the corresponding limit of the current-current response function.

The linear response theory yields the following equation for the electric current induced by the vector potential:

$$j_{\pm,\mu}(\mathbf{q}) = -\Pi_{\pm,\mu\nu}(\mathbf{q}) A_{\pm,\nu}(\mathbf{q}), \quad (36)$$

where  $A_{\pm,\nu}(\mathbf{q}) = A_{1,\nu}(\mathbf{q}) \pm A_{2,\nu}(\mathbf{q})$ , and

$$\Pi_{\pm,\mu\nu}(\mathbf{q}) = - \frac{1}{2cS} \int_0^\beta d\tau \langle T_\tau \hat{j}_{\pm,\mu}(\mathbf{q}, \tau) \hat{j}_{\pm,\nu}(-\mathbf{q}, 0) \rangle \quad (37)$$

is the current-current response function. In (37)  $\beta = 1/T$ ,  $T_\tau$  is the imaginary time ordering operator, and

$$\hat{j}_{\pm,\mu}(\mathbf{q}, \tau) = e^{H_{MF}\tau} \hat{j}_{\pm,\mu}(\mathbf{q}) e^{-H_{MF}\tau}.$$

As was already mentioned in Sec. III the current operator does not contain the diamagnetic term, different from the case considered in Ref. 1. We emphasize that it does not mean the absence of the diamagnetic effect. The diamagnetic response is included into the current-current response function.

The response functions (37) are similar to those that appear in the Bardeen-Cooper-Schrieffer (BCS) theory of superconductivity<sup>28</sup>. For the system of two monolayer graphenes it is equal to

$$\Pi_{\pm,\mu\nu}(\mathbf{q}) = - \frac{e^2 v_F^2}{c} \frac{\delta_{\mu\nu}}{S} \sum_{\sigma,\alpha,\lambda,\lambda',\mathbf{k}} F_{\nu,\lambda,\lambda',\mathbf{k},\mathbf{q}} \left[ P_{\lambda,\lambda',\mathbf{k},\mathbf{q}}^\pm \frac{1 - f_F(E_{\lambda',\mathbf{k}+\mathbf{q}}) - f_F(E_{\lambda,\mathbf{k}})}{E_{\lambda',\mathbf{k}+\mathbf{q}} + E_{\lambda,\mathbf{k}}} + L_{\lambda,\lambda',\mathbf{k},\mathbf{q}}^\pm \frac{f_F(E_{\lambda',\mathbf{k}+\mathbf{q}}) - f_F(E_{\lambda,\mathbf{k}})}{E_{\lambda,\mathbf{k}} - E_{\lambda',\mathbf{k}+\mathbf{q}}} \right], \quad (38)$$

where

$$F_{x,\lambda,\lambda',\mathbf{k},\mathbf{q}} = \frac{1 + \lambda\lambda' \cos(\theta_{\mathbf{k}+\mathbf{q}} + \theta_{\mathbf{k}})}{2}, \quad F_{y,\lambda,\lambda',\mathbf{k},\mathbf{q}} = \frac{1 - \lambda\lambda' \cos(\theta_{\mathbf{k}+\mathbf{q}} + \theta_{\mathbf{k}})}{2} \quad (39)$$

is the factor caused by the chirality of the graphene wave function,

$$P_{\lambda,\lambda',\mathbf{k},\mathbf{q}}^{\pm} = \frac{1}{2} \left( 1 - \frac{\xi_{\lambda',\mathbf{k}+\mathbf{q}}\xi_{\lambda,\mathbf{k}} \mp \Delta_{\lambda',\mathbf{k}+\mathbf{q}}\Delta_{\lambda,\mathbf{k}}}{E_{\lambda',\mathbf{k}+\mathbf{q}}E_{\lambda,\mathbf{k}}} \right), \quad (40)$$

$$L_{\lambda,\lambda',\mathbf{k},\mathbf{q}}^{\pm} = \frac{1}{2} \left( 1 + \frac{\xi_{\lambda',\mathbf{k}+\mathbf{q}}\xi_{\lambda,\mathbf{k}} \mp \Delta_{\lambda',\mathbf{k}+\mathbf{q}}\Delta_{\lambda,\mathbf{k}}}{E_{\lambda',\mathbf{k}+\mathbf{q}}E_{\lambda,\mathbf{k}}} \right) \quad (41)$$

are familiar in the BCS theory<sup>28</sup> coherence factors, and

$$f_F(E) = \frac{1}{\exp(E/T) + 1} \quad (42)$$

is the Fermi distribution function.

We will analyze the expression (38) in the constant gap approximation ( $\Delta_{\lambda,\mathbf{k}} = \Delta = \text{const}$ ) at  $T = 0$ . To obtain the London equation from (36) and (38) we consider the  $\mathbf{q} \rightarrow 0$  limit. Then the integral in (38) can be computed analytically:

$$\lim_{\mathbf{q} \rightarrow 0} \Pi_{+,xx}(\mathbf{q}) = -\frac{e^2}{2\pi\hbar^2 c} \epsilon_m \left[ \frac{\tilde{\epsilon}_m + 1}{\sqrt{(\tilde{\epsilon}_m + 1)^2 + \tilde{\Delta}^2}} + \frac{\tilde{\epsilon}_m - 1}{\sqrt{(\tilde{\epsilon}_m - 1)^2 + \tilde{\Delta}^2}} \right], \quad (43)$$

$$\begin{aligned} \lim_{\mathbf{q} \rightarrow 0} \Pi_{-,xx}(\mathbf{q}) = & -\frac{e^2}{2\pi\hbar^2 c} \epsilon_F \left[ \sqrt{(\tilde{\epsilon}_m + 1)^2 + \tilde{\Delta}^2} + \sqrt{(\tilde{\epsilon}_m - 1)^2 + \tilde{\Delta}^2} \right. \\ & \left. + \tilde{\Delta}^2 \ln \left( \frac{\sqrt{(\tilde{\epsilon}_m + 1)^2 + \tilde{\Delta}^2} + \tilde{\epsilon}_m + 1}{\sqrt{(\tilde{\epsilon}_m - 1)^2 + \tilde{\Delta}^2} + \tilde{\epsilon}_m - 1} \right) - 2\sqrt{1 + \tilde{\Delta}^2} - \tilde{\Delta}^2 \ln \left( \frac{\sqrt{1 + \tilde{\Delta}^2} + 1}{\sqrt{1 + \tilde{\Delta}^2} - 1} \right) \right]. \end{aligned} \quad (44)$$

Here  $\epsilon_m = \hbar v_F k_m$ , where  $k_m$  is the ultraviolet wave vector cutoff,  $\tilde{\epsilon}_m = \epsilon_m/\epsilon_F$ , and  $\tilde{\Delta} = \Delta/\epsilon_F$ . The quantities (43),(44) depend on the cut-off value  $k_m$ . That is the known shortage<sup>29</sup> of the linear approximation for the spectrum. This approximation is not valid in the whole Brillouin zone, while the correct answer can be obtained by the integration over the whole Brillouin zone.

The regularization of the answer (43),(44) is based on the requirement of the absence of the Meissner effect in the normal state. Due to noncommutativity of the limits  $T \rightarrow 0$  and  $\Delta \rightarrow 0$  we should return to Eq. (38). At  $\Delta = 0$  Eq. (38) is reduced to

$$\Pi_{+,\mu\nu}^0(\mathbf{q}) = \Pi_{-,\mu\nu}^0(\mathbf{q}) = -\frac{e^2 v_F^2}{c} \frac{\delta_{\mu\nu}}{S} \sum_{\sigma,\alpha,\lambda,\lambda',\mathbf{k}} F_{\nu,\lambda,\lambda',\mathbf{k},\mathbf{q}} \frac{f_F(\xi_{\lambda',\mathbf{k}+\mathbf{q}}) - f_F(\xi_{\lambda,\mathbf{k}})}{\xi_{\lambda,\mathbf{k}} - \xi_{\lambda',\mathbf{k}+\mathbf{q}}}. \quad (45)$$

From (45) we obtain

$$\lim_{\mathbf{q} \rightarrow 0} \Pi_{+,xx}^0(\mathbf{q}) = \lim_{\mathbf{q} \rightarrow 0} \Pi_{-,xx}^0(\mathbf{q}) = -\frac{e^2}{\pi\hbar^2 c} \epsilon_m. \quad (46)$$

The contribution of the rest of the Brillouin zone should compensate the quantity (46). The regularized response function is obtained by extracting from (43),(44) the quantity (46) and taking the limit  $\tilde{\epsilon}_m \rightarrow \infty$ . The result is

$$\lim_{\mathbf{q} \rightarrow 0} \Pi_{+,xx}^r(\mathbf{q}) = 0, \quad \lim_{\mathbf{q} \rightarrow 0} \Pi_{-,xx}^r(\mathbf{q}) = \frac{e^2}{\pi\hbar^2 c} \epsilon_F \left[ \sqrt{1 + \tilde{\Delta}^2} + \frac{\tilde{\Delta}^2}{2} \ln \left( \frac{\sqrt{1 + \tilde{\Delta}^2} + 1}{\sqrt{1 + \tilde{\Delta}^2} - 1} \right) \right]. \quad (47)$$

Substituting Eq. (47) into Eq. (36) and doing the reverse Fourier transformation we obtain the rigid relation between the supercurrent  $\mathbf{j}_-$  and the difference of the vector potentials  $\mathbf{A}_-$  in the form (34). As was expected, there is no rigid relation between  $\mathbf{j}_+$  and  $\mathbf{A}_+$ . The current  $\mathbf{j}_+$  is not connected with the motion of electron-hole pairs and it is not excited by the constant magnetic field. From (47) we see that the London rigidity depends on  $\Delta$ , different from the case of bulk superconductors, where the London rigidity at  $T = 0$  is determined by the electron density and independent of the BCS order parameter.

To obtain the superfluid stiffness we should take into account that the response function contains the contribution of four spin-valley components. The superfluid stiffness per the component is

$$\rho_s^m = \frac{1}{4} \frac{\hbar^2 c}{2e^2} \lim_{\mathbf{q} \rightarrow 0} \Pi_{-,xx}^r(\mathbf{q}) = \frac{\epsilon_F}{8\pi} \left[ \sqrt{1 + \tilde{\Delta}^2} + \frac{\tilde{\Delta}^2}{2} \ln \left( \frac{\sqrt{1 + \tilde{\Delta}^2} + 1}{\sqrt{1 + \tilde{\Delta}^2} - 1} \right) \right]. \quad (48)$$

For  $\Delta \ll \epsilon_F$  the superfluid stiffness  $\rho_s = \epsilon_F/8\pi$ , which coincides with the result of Ref. 30.

For the system of two bilayer graphenes the response functions  $\Pi_{\pm,xx}$  are given by the equation

$$\Pi_{\pm,xx}(\mathbf{q}) = -\frac{e^2 \hbar^2}{m^2 c S} \sum_{\sigma, \alpha, \lambda, \lambda', \mathbf{k}} G_{\lambda, \lambda', \mathbf{k}, \mathbf{q}}^{xx} \left[ P_{\lambda, \lambda', \mathbf{k}, \mathbf{q}}^{\pm} \frac{1 - f_F(E_{\lambda', \mathbf{k} + \mathbf{q}}) - f_F(E_{\lambda, \mathbf{k}})}{E_{\lambda', \mathbf{k} + \mathbf{q}} + E_{\lambda, \mathbf{k}}} + L_{\lambda, \lambda', \mathbf{k}, \mathbf{q}}^{\pm} \frac{f_F(E_{\lambda', \mathbf{k} + \mathbf{q}}) - f_F(E_{\lambda, \mathbf{k}})}{E_{\lambda, \mathbf{k}} - E_{\lambda', \mathbf{k} + \mathbf{q}}} \right], \quad (49)$$

where

$$G_{\lambda, \lambda', \mathbf{k}, \mathbf{q}}^{xx} = \left( k_x + \frac{q_x}{2} \right)^2 \frac{1 + \lambda \lambda' \cos[2(\theta_{\mathbf{k} + \mathbf{q}} + \theta_{\mathbf{k}})]}{2} + \left( k_y + \frac{q_y}{2} \right)^2 \frac{1 - \lambda \lambda' \cos[2(\theta_{\mathbf{k} + \mathbf{q}} + \theta_{\mathbf{k}})]}{2} + \lambda \lambda' \left( k_x + \frac{q_x}{2} \right) \left( k_y + \frac{q_y}{2} \right) \sin[2(\theta_{\mathbf{k} + \mathbf{q}} + \theta_{\mathbf{k}})]. \quad (50)$$

The calculation yields the answer that also depends on the ultraviolet cutoff. To regularize the answer we should extract the quantity  $\lim_{\mathbf{q} \rightarrow 0} \Pi_{\pm,xx}^0(\mathbf{q})$ , where

$$\Pi_{\pm,xx}^0(\mathbf{q}) = -\frac{e^2 \hbar^2}{m^2 c S} \sum_{\sigma, \alpha, \lambda, \lambda', \mathbf{k}} G_{\lambda, \lambda', \mathbf{k}, \mathbf{q}}^{xx} \frac{f_F(\xi_{\lambda', \mathbf{k} + \mathbf{q}}) - f_F(\xi_{\lambda, \mathbf{k}})}{\xi_{\lambda, \mathbf{k}} - \xi_{\lambda', \mathbf{k} + \mathbf{q}}} \quad (51)$$

is the response function in the normal state. It yields the response function  $\Pi_{-,xx}$  that in the limit  $\mathbf{q} \rightarrow 0$  differs from the function (47) by the factor of 2. The superfluid stiffness per the spin-valley component is

$$\rho_s^b = \frac{\epsilon_F}{4\pi} \left[ \sqrt{1 + \tilde{\Delta}^2} + \frac{\tilde{\Delta}^2}{2} \ln \left( \frac{\sqrt{1 + \tilde{\Delta}^2} + 1}{\sqrt{1 + \tilde{\Delta}^2} - 1} \right) \right]. \quad (52)$$

For  $\Delta \ll \epsilon_F$  the superfluid stiffness  $\rho_s = \epsilon_F/4\pi$ , which coincides with the phenomenological expression (35) in which  $n$  is the electron (hole) density per the component and  $M = 2m$ .

Equations (44) and (52) are the main result of this section. We find that the zero-temperature superfluid stiffness increases under increase in  $\Delta$ . In the small gap limit this quantity is determined entirely by the density of carriers in the conduction band.

Let us now evaluate the value of the diamagnetic effect. The diamagnetic susceptibility is determined by the ratio of the magnetization, induced by the current  $\mathbf{j}_-$ , to the external magnetic field. For  $\mathbf{B}$  directed parallel to the graphene layers  $A_{1,x} - A_{2,x} = B_y d$ , and

$$\chi = \frac{1}{4\pi} \frac{2\pi j_{-,x}}{c B_y} = -\frac{d}{2c} \lim_{q \rightarrow 0} \Pi_{-,xx}^r(q). \quad (53)$$

It yields

$$\chi^m \approx -\frac{1}{2\pi} \left( \frac{e^2}{\hbar c} \right)^2 \frac{1}{\alpha_{eff}} k_F d \quad (54)$$

for the system of two monolayer graphenes, and

$$\chi^b \approx -\frac{1}{2\pi} \left( \frac{e^2}{\hbar c} \right)^2 k_F^2 d a_B^{eff} \quad (55)$$

for the system of two bilayer graphenes. Here  $\alpha_{eff} = e^2/\hbar v_F \approx 2.2$  is the effective fine-structure constant for the monolayer graphene,  $a_B^{eff} = \hbar^2/m\epsilon^2 \approx 1.5$  nm is the effective Bohr radius for the bilayer graphene, and  $k_F$  is the Fermi wave vector. In these estimates we neglect the dependence of the London rigidity on  $\Delta/\epsilon_F$ .

The diamagnetic effect can be observed in a multiple-connected system (a double layer Corbino disk, a double layer hollow cylinder). The effect is maximal at zero temperature and it vanishes in the normal state. The current induced by the external magnetic field can be rather large. Taking, for instance,  $B = 0.1$  T,  $\epsilon_F = 0.1$  eV, and  $d = 5$  nm, we obtain the density of the current  $j_- \sim 1$  A/m. At the same time the diamagnetic susceptibility, which is proportional to the square of the fine-structure constant, is small ( $4\pi\chi \sim 10^{-6} - 10^{-5}$ ). Moreover, the magnetic field, induced by the current  $j_-$ , emerges only in a narrow dielectric layer that separates two graphene sheets. Therefore, it is a hard task to register this diamagnetic effect in the magnetic measurements.



## V. SUPPRESSION OF SCREENING CAUSED BY THE ELECTRON-HOLE PAIRING

Taking into account the smallness of the diamagnetic effect it is desirable to find another effect that can be used as an indicator of the superconductive transition. In this section we consider screening of the electric field of a test charge. We imply that the system (Fig. 1) consists of two monolayer or two bilayer graphene sheets, separated by a dielectric layer. The system is suspended in dielectric medium with the dielectric constant close to unity.

The electrostatic potential applied to the bilayer system results in the appearance of the induced charges in graphene sheets  $e\rho_{\pm}^{ind} = e(\rho_1^{ind} \pm \rho_2^{ind})$ . They can be expressed through the single particle density-density response functions:

$$e\rho_{\pm}^{ind}(\mathbf{q}) = e^2\Pi_{\pm}(\mathbf{q})\varphi_{\pm}(\mathbf{q}), \quad (56)$$

where

$$\Pi_{\pm}(\mathbf{q}) = -\frac{1}{2S} \int_0^{\beta} d\tau \langle T_{\tau} \hat{\rho}_{\pm}(\mathbf{q}, \tau) \hat{\rho}_{\pm}(-\mathbf{q}, 0) \rangle, \quad (57)$$

$\varphi_{\pm}(\mathbf{q}) = \varphi_1(\mathbf{q}) \pm \varphi_2(\mathbf{q})$ , and  $\varphi_i(\mathbf{q})$  is the two-dimensional Fourier component of the scalar potential  $\varphi(\mathbf{r})$  in the layer  $i$ . The potential  $\varphi(\mathbf{r})$  should be found self-consistently. It is the sum of the bare potential created by the test charge, and the potential caused by the induced charges. The potential  $\varphi(\mathbf{r})$  satisfies the equation

$$\nabla [\varepsilon(z)\nabla\varphi(\mathbf{r})] = -4\pi [Q\delta(\mathbf{r} - \mathbf{r}_Q) + e\rho_1^{ind}(\mathbf{r}_{\perp})\delta(z - z_1) + e\rho_2^{ind}(\mathbf{r}_{\perp})\delta(z - z_2)]. \quad (58)$$

In (58) we consider the test charge  $Q = Ze$  located at the point  $\mathbf{r}_Q = (\mathbf{r}_{Q\perp}, z_Q)$ : the axis  $z$  is directed perpendicular to the graphene layers,  $z_1$  and  $z_2$  are the coordinates of the graphene layers, and  $\mathbf{r}_{\perp}$  is the two-dimensional radius vector. We put  $z_Q > z_1 > z_2$  and

$$\varepsilon(z) = \begin{cases} \varepsilon, & z_2 < z < z_1 \\ 1, & \text{otherwise.} \end{cases}$$

The solution of Eq. (58) yields

$$e\varphi_i(\mathbf{q}) = ZV_{iQ}(q) + \sum_j V_{ij}(q)\rho_j^{ind}(\mathbf{q}), \quad (59)$$

where

$$V_{11}(q) = V_{22}(q) = \frac{4\pi e^2}{q} \frac{(\varepsilon + 1) + (\varepsilon - 1)e^{-2qd}}{(\varepsilon + 1)^2 - e^{-2qd}(\varepsilon - 1)^2}, \quad V_{12}(q) = V_{21}(q) = \frac{8\pi e^2}{q} \frac{\varepsilon e^{-qd}}{(\varepsilon + 1)^2 - e^{-2qd}(\varepsilon - 1)^2} \quad (60)$$

are the potentials of interaction of elementary charges located in the graphene layers,  $d = |z_1 - z_2|$  is the distance between the graphene layers,  $V_{iQ}(q) = e^{-qa}V_{i1}(q)$  is the potential of interaction between the elementary test charge and the induced charge in the  $i$ th layer, and  $a = |z_Q - z_1|$  is the distance from the test charge to the nearest graphene layer. Substituting (59) into (56) we obtain the induced charges

$$\rho_{\pm}^{ind}(\mathbf{q}) = Ze^{-qa} \frac{V_{\pm}(q)\Pi_{\pm}(\mathbf{q})}{1 - V_{\pm}(q)\Pi_{\pm}(\mathbf{q})}, \quad (61)$$

where

$$V_{\pm}(q) = V_{11}(q) \pm V_{12}(q) = \frac{4\pi e^2}{q} \frac{1 \pm e^{-qd}}{(\varepsilon + 1) \mp (\varepsilon - 1)e^{-qd}}. \quad (62)$$

Substituting the induced charges (61) into Eq. (58) and solving it we obtain the expression for the screened potential  $\varphi(\mathbf{r})$  as the linear function of the test charge  $Q$ .

We consider the cases (see Fig. 1) where the electric field sensor is located at the side of the test charge [point P with the coordinate  $\mathbf{r}_P = (\mathbf{r}_{Q\perp} + \mathbf{r}_{\perp}, z_Q)$ ] or at the opposite side [point P' with the coordinate  $\mathbf{r}_{P'} = (\mathbf{r}_{Q\perp}, z_Q - z)$ , where  $z > a + d$ ].

At the point P the potential is given by the equation

$$\varphi_P(r) = \frac{Q}{r} - Q \int_0^{\infty} dq J_0(qr) e^{-2qa} \left[ \frac{(\varepsilon^2 - 1)(1 - e^{-2qd})}{(\varepsilon + 1)^2 - e^{-2qd}(\varepsilon - 1)^2} - \frac{q}{4\pi e^2} \left( \frac{V_+^2(q)\Pi_+(q)}{1 - V_+(q)\Pi_+(q)} - \frac{V_-^2(q)\Pi_-(q)}{1 - V_-(q)\Pi_-(q)} \right) \right], \quad (63)$$

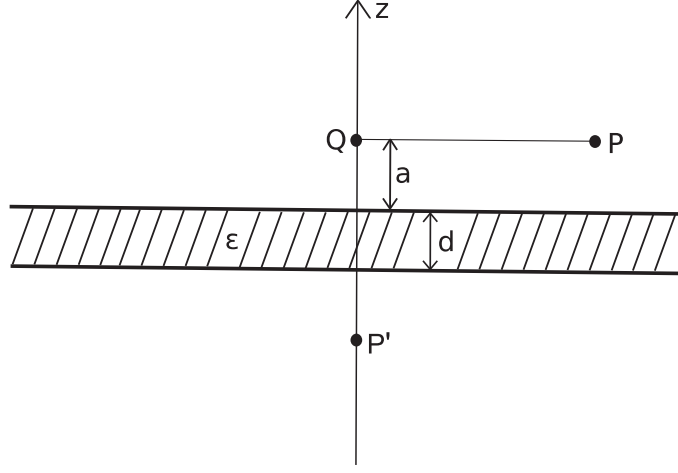


FIG. 1: Schematic view of the system under consideration.

where  $J_0(x)$  is the Bessel function. The potential at the point  $P'$  is equal to

$$\varphi_{P'}(z) = Q \int_0^\infty dq e^{-qz} \left[ \frac{4\varepsilon}{(\varepsilon + 1)^2 - e^{-2qd}(\varepsilon - 1)^2} + \frac{qe^{qd}}{4\pi e^2} \left( \frac{V_+^2(q)\Pi_+(q)}{1 - V_+(q)\Pi_+(q)} - \frac{V_-^2(q)\Pi_-(q)}{1 - V_-(q)\Pi_-(q)} \right) \right]. \quad (64)$$

In (63) and (64) we take into account that  $\Pi_\pm(\mathbf{q})$  is the function of the modulus of the wave vector.

The density-density response function is computed analogously to the current-current response function. The answer is

$$\Pi_\pm(\mathbf{q}) = -\frac{1}{S} \sum_{\sigma, \alpha, \lambda, \lambda', \mathbf{k}} F_{\lambda, \lambda', \mathbf{k}, \mathbf{q}}^{m(b)} \left[ P_{\lambda, \lambda', \mathbf{k}, \mathbf{q}}^\mp \frac{1 - f_F(E_{\lambda', \mathbf{k} + \mathbf{q}}) - f_F(E_{\lambda, \mathbf{k}})}{E_{\lambda', \mathbf{k} + \mathbf{q}} + E_{\lambda, \mathbf{k}}} + L_{\lambda, \lambda', \mathbf{k}, \mathbf{q}}^\mp \frac{f_F(E_{\lambda', \mathbf{k} + \mathbf{q}}) - f_F(E_{\lambda, \mathbf{k}})}{E_{\lambda, \mathbf{k}} - E_{\lambda', \mathbf{k} + \mathbf{q}}} \right], \quad (65)$$

where the chirality factors  $F_{\lambda, \lambda', \mathbf{k}, \mathbf{q}}^{m(b)}$  are given by Eq. (23), and the coherence factors  $P^\pm$  and  $L^\pm$ , by Eq. (40) and (41). The response functions (65) do not depend on the ultraviolet cutoff and do not require regularization.

We note that Eqs. (63)-(65) correspond to the random phase approximation (RPA) and do not account the vertex corrections. It is known that in the BCS theory the vertex corrections are important for obtaining the gauge-invariant result<sup>28</sup>. The same is true for the electron-hole pairing. Fortunately, the problem with the gauge invariance does not emerge under computation of the density response function in the static limit. Nevertheless, one can ask about the value of the vertex corrections. This problem was addressed in Ref. 31 where the electron-hole pairing in bilayer systems with the quadratic spectrum of carriers (double quantum wells is GaAs heterostructures) was studied. The good agreement between the RPA<sup>31</sup> and the diffusion quantum Monte Carlo<sup>32,33</sup> computations for the condensate fraction allows the authors of Ref. 31 to conclude that the vertex corrections are negligible. The vertex corrections for the graphene systems with electron-hole pairing were evaluated in Ref. 15. It was shown<sup>15</sup> that the second-order vertex corrections amount only to about 5% of the first-order coupling constants and thus can be neglected. The general argument for neglecting the vertex corrections in the graphene system is that they are small by the factor  $1/N$ , where  $N$  is number of electron flavors ( $N = 4$  corresponds to four spin-valley components).

Let us return to Eqs. (63)-(65) and consider first the  $T = 0$  case. The dependencies  $\Pi_\pm(q)$  at  $T = 0$  and  $\Delta = const$  are shown in Figs. 2 and 3 for the system of two monolayer and two bilayer graphenes, correspondingly. In the normal state ( $\Delta = 0$ ) the response functions  $\Pi_+$  and  $\Pi_-$  are equal to each other and coincide with the response function for the monolayer<sup>34,35</sup> (bilayer<sup>36</sup>) graphene. In the limit  $qk_F \ll 1$  they approach  $\Pi_+(0) = \Pi_-(0) = N_F^{m(b)}$ , the density of states of the monolayer (bilayer) graphene at the Fermi level ( $N_F^m = 2k_F/\pi\hbar v_F$  and  $N_F^b = 2m/\pi\hbar^2$ ). In the superconductive state ( $\Delta \neq 0$ ) the response function  $\Pi_+$  approaches zero at  $q \rightarrow 0$ . It principally changes the character of screening.

In the normal state the scalar potential  $\varphi_P(r)$  at  $d \lesssim k_F^{-1} \ll a \ll r$  has the universal asymptote

$$\varphi_P(r) \approx \frac{2Qa^2}{r^3}. \quad (66)$$

Actually, it is the potential of a dipole consisting of the test charge and its image. In the superconductive state the

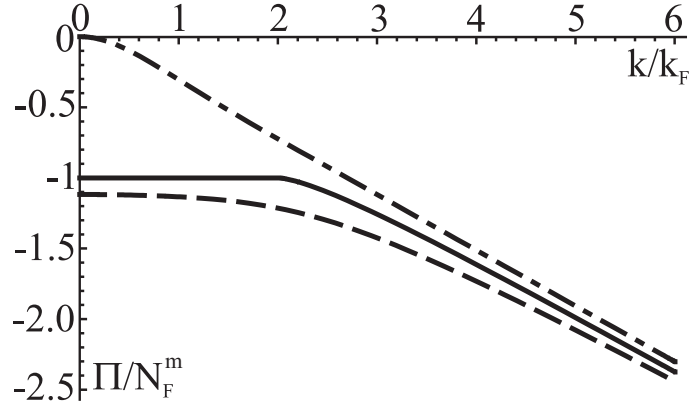


FIG. 2: The density response functions  $\Pi_+$  (dash-dotted line),  $\Pi_-$  (dashed line) in the superconductive state (for  $\Delta = 0.5\epsilon_F$ ), and  $\Pi = \Pi_{\pm}$  (solid line) in the normal state for the system of two monolayer graphenes.

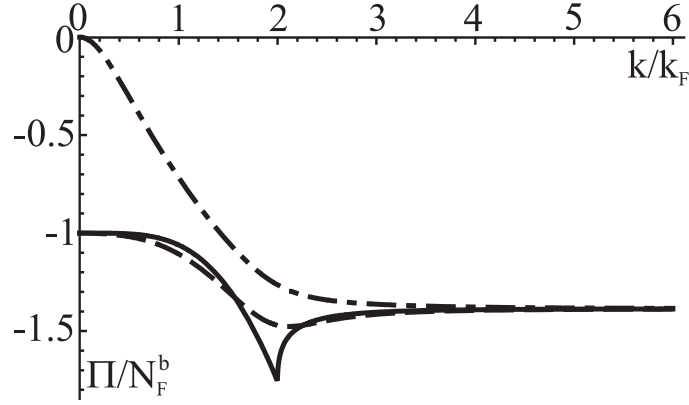


FIG. 3: The same as in Fig. 2 for the system of two bilayer graphenes.

second term in (63) yields only  $1/r^3$  correction and the scalar potential remains unscreened at large  $r$  :

$$\varphi_P(r) \approx \frac{Q}{r}.$$

Similar features demonstrates the potential  $\varphi_{P'}(z)$ . In the normal state its asymptote is

$$\varphi_{P'}(z) = \frac{Q}{k_F z^2} \frac{1}{8\alpha_{eff} \left(1 + \frac{4\alpha_{eff} dk_F}{\epsilon}\right)} \quad (67)$$

(for the system of two monolayer graphenes) and

$$\varphi_{P'}(z) = \frac{Q a_B^{eff}}{z^2} \frac{1}{8 \left(1 + \frac{4d}{\epsilon a_B^{eff}}\right)} \quad (68)$$

(for the system of two bilayer graphenes). In the superconductive state the potential remains unscreened at large  $z$  [ $\varphi_{P'}(z) = Q/z$ ].

For  $T \neq 0$ ,  $T \ll \Delta$  the function  $\Pi_+(q)$  at  $q \rightarrow 0$  approaches a small ( $\propto e^{-\Delta/T}$ ) but finite value. It changes the character of screening at very large distances. The asymptotes are  $\varphi_P(r) = C/r^3$ , and  $\varphi_{P'}(z) = C'/z^2$ , but the coefficients of proportionality  $C$  and  $C'$  contain the large factor  $e^{\Delta/T}$ . At  $T \gg \Delta$  the screening in the superconductive state is almost the same as in the normal state. The screened potential at intermediate distance to the test charge is shown in Fig. 4 [screening along the structure, the potential  $\varphi_P(r)$ ] and Fig. 5 [screening across the structure, the potential  $\varphi_{P'}(z)$ ]. The parameters  $\Delta = 0.5\epsilon_F$ ,  $dk_F = 0.2$ ,  $a_B^{eff} k_F = 0.25$ , and  $ak_F = 4$  are used for the computation.

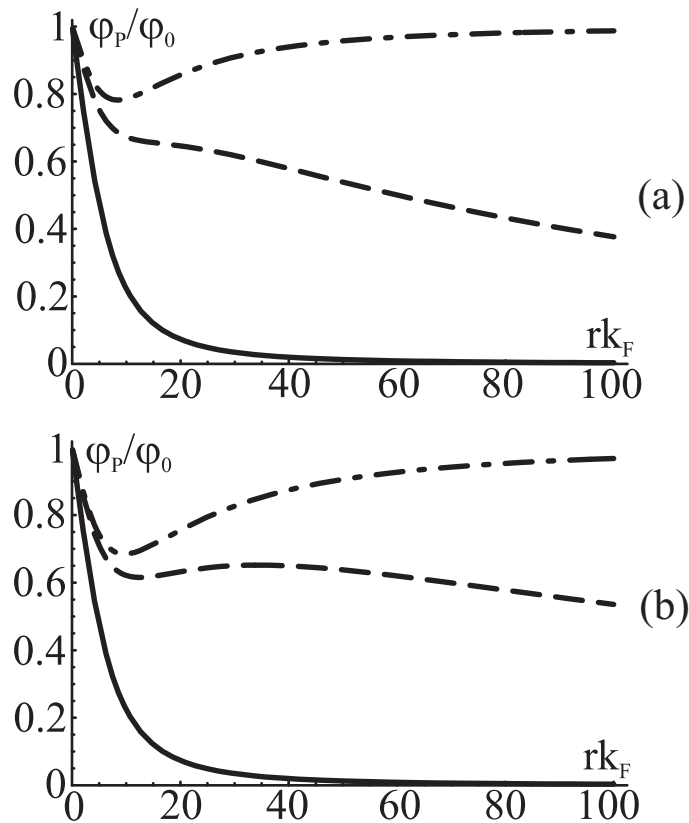


FIG. 4: Screening along the structure of two monolayer (a) and two bilayer (b) graphenes in the normal state (solid line), and in the superconductive state at  $T = 0$  (dash-dotted line) and  $T = 0.1\Delta$  (dashed line). The potential is normalized to the bare potential  $\varphi_0 = Q/r$ .

One can see that the electron-hole pairing essentially changes the spatial dependence of the screened potential both at zero and at finite temperatures.

Thus we conclude that the electron-hole pairing reveals itself in spectacular changes of the electric field of the test charge located near the double layer system. The effect can be used as an indicator of the electron-hole pairing.

The most effective method of measuring the local electrostatic potential uses the single-electron transistor (SET) technique. Operating at low temperature the SET scanning electrometer is capable of measuring the potential with millivolt<sup>37</sup> to microvolt<sup>38</sup> sensitivity a high spatial resolution close to the SET size (about 100 nm). A quantum-metrology technique for precision three-dimensional electric-field measurement using a single nitrogen-vacancy defect center spin in diamond was also developed<sup>39</sup>. While it is less sensitive than SET, it allows measuring the field created by an elementary charge located at a distance less or about 150 nm from the sensor. The latter technique does not require low temperature. Thus the electrostatic method of registration of the electron-hole pairing is doable with the current technologies.

## VI. CONCLUSION

In conclusion we have shown that in the double layer graphene system the electron-hole pairing results in the Meissner effect and in the strong suppression of screening of the test charge. The effects demonstrate the same temperature behavior. They are maximal at zero temperature, decrease under increase in the temperature, and disappear in the normal state. It is connected with the similarity of the current-current and density-density response functions. Such a similarity is specific for the electron-hole pairing. It does not occur in superconductors with the electron-electron pairing. The Meissner effect in the system under study is extremely small and most probably it cannot be used as an indicator of the electron-hole pairing. On the other hand, the suppression of screening is strong and the observation of this effect can be used as a hallmark of the transition into the superconductive state.

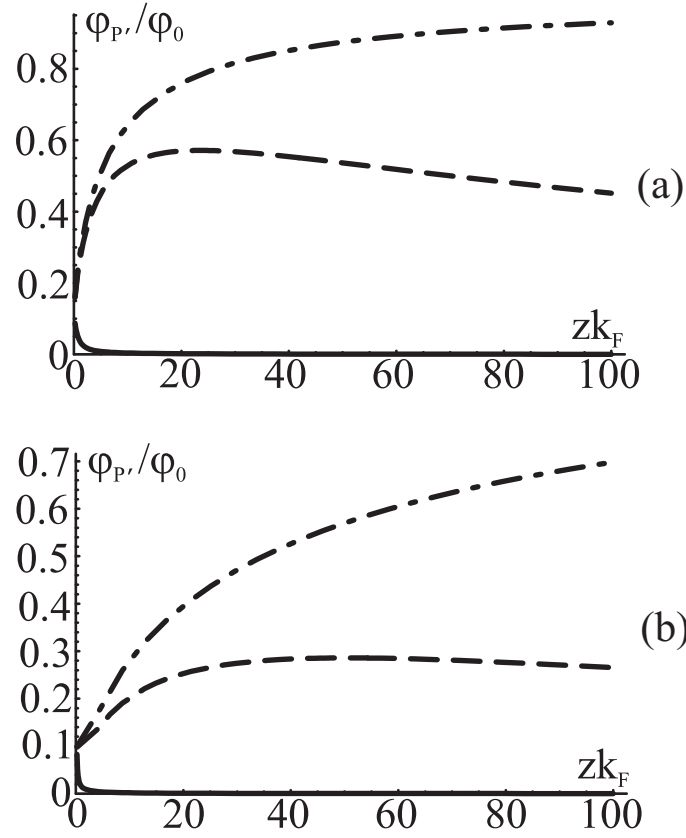


FIG. 5: The same as in Fig. 4 for the screening across the structure. The potential is normalized to  $\varphi_0 = Q/z$ .

#### Acknowledgment

This work was supported by the Ukraine State Scientific and Technical Program "Nanotechnologies and nanomaterials".

- 
- <sup>1</sup> S. I. Shevchenko, *Fiz. Nizk. Temp.* **2**, 505 (1976) [*Sov. J. Low Temp. Phys.* **2**, 251 (1976)].  
<sup>2</sup> Yu. E. Lozovik and V. I. Yudson, *Zh. Eksp. Teor. Fiz.* **71**, 738 (1976) [*Sov. Phys. JETP* **44**, 389 (1976)].  
<sup>3</sup> H. A. Fertig, *Phys. Rev. B* **40**, 1087 (1989).  
<sup>4</sup> D. Yoshioka and A. H. MacDonald, *J. Phys. Soc. Jpn.* **59**, 4211 (1990).  
<sup>5</sup> K. Moon, H. Mori, K. Yang, S. M. Girvin, A. H. MacDonald, L. Zheng, D. Yoshioka, and S. C. Zhang, *Phys. Rev. B* **51**, 5138 (1995).  
<sup>6</sup> M. Kellogg, J. P. Eisenstein, L. N. Pfeiffer, and K. W. West, *Phys. Rev. Lett.* **93**, 036801 (2004).  
<sup>7</sup> R. D. Wiersma, J. G. S. Lok, S. Kraus, W. Dietsche, K. von Klitzing, D. Schuh, M. Bichler, H.-P. Tranitz, and W. Wegscheider, *Phys. Rev. Lett.* **93**, 266805 (2004).  
<sup>8</sup> E. Tutuc, M. Shayegan, and D. A. Huse, *Phys. Rev. Lett.* **93**, 036802 (2004).  
<sup>9</sup> D. Nandi, A. D. K. Finck, J. P. Eisenstein, L. N. Pfeiffer, K. W. West, *Nature (London)* **488**, 481 (2012).  
<sup>10</sup> Yu. E. Lozovik and A. A. Sokolik, *Pisma Zh. Eksp. Teor. Fiz.* **87**, 61 (2008) [*JETP Lett.* **87**, 55 (2008)].  
<sup>11</sup> H. Min, R. Bistritzer, J.-J. Su, and A. H. MacDonald, *Phys. Rev. B* **78**, 121401(R) (2008).  
<sup>12</sup> B. Seradjeh, H. Weber, and M. Franz, *Phys. Rev. Lett.* **101**, 246404 (2008).  
<sup>13</sup> M. Y. Kharitonov and K. B. Efetov, *Phys. Rev. B* **78**, 241401(R) (2008); *Semicond. Sci. Technol.* **25**, 034004 (2010).  
<sup>14</sup> I. Sodemann, D. A. Pesin, and A. H. MacDonald, *Phys. Rev. B* **85**, 195136 (2012).  
<sup>15</sup> Yu. E. Lozovik, S. L. Ogarkov, and A. A. Sokolik, *Phys. Rev. B* **86**, 045429 (2012).  
<sup>16</sup> A. Perali, D. Neilson, and A. R. Hamilton, *Phys. Rev. Lett.* **110**, 146803 (2013).  
<sup>17</sup> M. Zarenia, A. Perali, D. Neilson, and F. M. Peeters, *Sci. Rep.* **4**, 7319 (2014).  
<sup>18</sup> A. F. Croxall, K. Das Gupta, C. A. Nicoll, M. Thangaraj, H. E. Beere, I. Farrer, D.A. Ritchie, and M. Pepper, *Phys. Rev. Lett.* **101**, 246801 (2008).

- <sup>19</sup> J. A. Seamons, C. P. Morath, J. L. Reno, and M. P. Lilly, Phys. Rev. Lett. **102** 026804 (2009).
- <sup>20</sup> A. Gamucci, D. Spirito, M. Carrega, B. Karmakar, A. Lombardo, M. Bruna, L.N. Pfeiffer, K.W. West, A.C. Ferrari, M. Polini, and V. Pellegrini, Nat. Commun. **5**, 5824 (2014).
- <sup>21</sup> R. V. Gorbachev, A. K. Geim, M. I. Katsnelson, K. S. Novoselov, T. Tudorovskiy, I. V. Grigorieva, A. H. MacDonald, S. V. Morozov, K. Watanabe, T. Taniguchi, and L. A. Ponomarenko, Nat. Phys. **8**, 896 (2012).
- <sup>22</sup> A. H. Castro Neto, F. Guinea, N. M. R. Peres, K. S. Novoselov, and A. K. Geim, Rev. Mod. Phys. **81**, 109 (2009).
- <sup>23</sup> Y. Nambu, Phys. Rev. **117**, 648 (1960).
- <sup>24</sup> A. V. Balatsky, Y. N. Joglekar, and P. B. Littlewood, Phys. Rev. Lett. **93**, 266801 (2004).
- <sup>25</sup> S. I. Shevchenko, Phys. Rev. B **56**, 10355 (1997).
- <sup>26</sup> E. B. Sonin, Phys. Rev. Lett. **102**, 106407 (2009).
- <sup>27</sup> J. M. Kosterlitz and D. J. Thouless, J. Phys. C **5**, L124 (1972).
- <sup>28</sup> J. R. Schrieffer, Theory of Superconductivity (Benjamin, New York, 1964).
- <sup>29</sup> A. Principi, M. Polini, and G. Vignale, Phys. Rev. B **80**, 075418 (2009).
- <sup>30</sup> D. K. Efimkin, V. A. Kulbachinskii, and Yu. E. Lozovik, Pis'ma Zh. Eksp. Teor. Fiz. **93**, 238 (2011) [JETP Lett. **93**, 219 (2011)].
- <sup>31</sup> D. Neilson, A. Perali, and A. R. Hamilton, Phys. Rev. B **89**, 060502(R) (2014).
- <sup>32</sup> R. Maezono, P. Lopez Rios, T. Ogawa, and R. J. Needs, Phys. Rev. Lett. **110**, 216407 (2013).
- <sup>33</sup> S. De Palo, F. Rapisarda, and G. Senatore, Phys. Rev. Lett. **88**, 206401 (2002).
- <sup>34</sup> T. Ando, J. Phys. Soc. Jpn. **75**, 074716 (2006).
- <sup>35</sup> E.H. Hwang and S. Das Sarma, Phys. Rev. B **75**, 205418 (2007).
- <sup>36</sup> E. H. Hwang and S. Das Sarma, Phys. Rev. Lett. **101**, 156802 (2008).
- <sup>37</sup> M. J. Yoo, T. A. Fulton, H. F. Hess, R. L. Willett, L. N. Dunkleberger, R. J. Chichester, L. N. Pfeiffer, and K. W. West, Science **276**, 579 (1997).
- <sup>38</sup> J. Martin, N. Akerman, G. Ulbricht, T. Lohmann, J. H. Smet, K. von Klitzing, and A. Yacoby, Nat. Phys. **4**, 144 (2008).
- <sup>39</sup> F. Dolde, H. Fedder, M.W. Doherty, T. Nobauer, F. Rempp, G. Balasubramanian, T. Wolf, F. Reinhard, L. C. L. Hollenberg, F. Jelezko, and J. Wrachtrup, Nat. Phys. **7**, 459 (2011).